1-1-2019

A simple technique for development of fibres with programmable microsphere concentration gradients for local protein delivery

Fahimeh Mehrpouya
University of Wollongong, fm392@uowmail.edu.au

Zhilian Yue
University of Wollongong, zyue@uow.edu.au

Anthony C. Romeo
University of Wollongong, tromeo@uow.edu.au

Robert A. Gorkin III
University of Wollongong, rgorkin@uow.edu.au

Robert M. I Kapsa
University of Wollongong, robk@uow.edu.au

See next page for additional authors

A simple technique for development of fibres with programmable microsphere concentration gradients for local protein delivery

Abstract

Alginate has been a biologically viable option for controlled local delivery of bioactive molecules in vitro and in vivo. Specific bioactive molecule release profiles are achieved often by controlling polymer composition/concentration, which also determines the modulus of hydrogels. This largely limits alginate-mediated bioactive molecule delivery to single-factors of uniform concentration applications, rather than applications that may require (multiple) bioactive molecules delivered at a concentration gradient for chemotactic purposes. Here we report a two-phase PLGA/alginate delivery system composed of protein-laden poly-d,l-lactic-co-glycolic acid (PLGA) microspheres wet-spun into alginate fibres. Fluorescein isothiocyanate-conjugated bovine serum albumin (FITC-BSA) was used as a model protein and the developed structures were characterized. The fabrication system devised was shown to produce wet-spun fibres with a protein concentration gradient (G-Alg/PLGA fibre). The two-phase delivery matrices display retarded FITC-BSA release in both initial and late stages compared to release from the PLGA microspheres or alginate fibre alone. In addition, incorporation of higher concentrations of protein-loaded PLGA microspheres increased protein release compared to the fibres with lower concentrations of BSA-loaded microspheres. The "programmable" microsphere concentration gradient fibre methodology presented here may enable development of novel alginate scaffolds with the ability to guide tissue regeneration through tightly-controlled release of one or more proteins in highly defined spatio-temporal configurations.

Disciplines

Engineering | Physical Sciences and Mathematics

Publication Details

Mehrpouya, F., Yue, Z., Romeo, T., Gorkin, R., Kapsa, R. M. I., Moulton, S. E. & Wallace, G. G. (2019). A simple technique for development of fibres with programmable microsphere concentration gradients for local protein delivery. Journal of Materials Chemistry B, 7 (4), 556-565.

Authors

Fahimeh Mehrpouya, Zhilian Yue, Anthony C. Romeo, Robert A. Gorkin III, Robert M. I Kapsa, Simon E. Moulton, and Gordon G. Wallace

A simple technique for development of fibres with programmable microsphere concentration gradients for local protein delivery

Fahimeh Mehrpouya,[a] Zhilian Yue,[*a] Tony Romeo,[b] Robert Gorkin,[a]

Robert M.I. Kapsa,[a,c] Simon E. Moulton,[d] Gordon G. Wallace[*a]

[a]Intelligent Polymer Research Institute,

ARC Centre of Excellence for Electromaterials Science,

AIIM Facility, Innovation Campus, University of Wollongong, NSW 2522, Australia.

[b]UOW Electron Microscopy Centre, Innovation Campus, University of Wollongong,

NSW 2522, Australia

[c]BioFab3D, St. Vincent's Hospital Melbourne, Victoria 3065, Australia.

[d]Swinburne University of Technology,

ARC Centre of Excellence for Electromaterials Science,

VIC 3122, Australia.

*Correspondence. Zhilian Yue, Intelligent Polymer Research Institute, ARC Centre of Excellence for Electromaterials Science, AIIM Facility, Innovation Campus, University of Wollongong, Wollongong, New South Wales 2522, Australia. E-mail: zyue@uow.edu.au; Tel: +61-2-42213832. Gordon G. Wallace, Intelligent Polymer Research Institute, ARC Centre of Excellence for Electromaterials Science, AIIM Facility, Innovation Campus, University of Wollongong, Wollongong, New South Wales 2522, Australia. E-mail: gwallace@uow.edu.au; Tel: +61-2-42213127.

Abstract:

Alginate has been a biologically viable option for controlled local delivery of bioactive molecules in vitro and in vivo. Specific bioactive molecule release profiles are achieved often by controlling polymer composition/concentration, which also determines the modulus of hydrogel. This largely limits alginate-mediated bioactive molecule delivery to single-factors of uniform concentration applications, rather than applications that may require (multiple) bioactive molecules delivered at a concentration gradient for chemotactic purposes. Here we report a two-phase PLGA/alginate delivery system composed of protein-laden poly D, L-lactic-co-glycolic acid (PLGA) microspheres wet-spun into alginate fibres. Fluorescein isothiocyanate-conjugated bovine serum albumin (FITC-BSA) was used as a model protein and the developed structures were characterized. The fabrication system devised was shown to produce wet-spun fibres with a protein concentration gradient (G-Alg/PLGA fibre). The two-phase delivery matrices display retarded FITC-BSA release in both initial and late stages compared to release from the PLGA microspheres or alginate fibre alone. In addition, incorporation of higher concentrations of protein-loaded PLGA microspheres increased protein release compared to the fibres with lower concentrations of BSA-loaded microspheres. The "programmable" microspheres concentration gradient fibre methodology presented here may enable development of novel alginate scaffolds with the ability to guide tissue regeneration through tightly-controlled release of one or more proteins in highly defined spatio-temporal configurations

Keywords:

Controlled protein release, alginate fibre, PLGA microspheres, programmable local delivery, concentration gradient.

Introduction

Over the past two decades, localized delivery of therapeutic proteins such as protein drugs and growth factors to dysfunctional or damaged soft tissues has gained significant importance to a number of biomedical areas, particularly in tissue engineering applications.[1] Localized delivery systems overcome the drawbacks associated with systematic approaches wherein distribution of therapeutic molecules via the circulatory system often results in diffuse efficacy and side-effects in non-target tissues.[2,3] Therefore, fabrication of effective and versatile protein delivery systems is important to most, if not all, bioactive molecule delivery, pharmaceutics, and tissue engineering applications.[4,5] From this viewpoint, the general biocompatibility and hydrophilic nature of alginate (Alg) based structures has made Alg one of the most common platforms being investigated for therapeutic protein delivery.[6-8]

A critical challenge in the field of bioactive molecules delivery in tissue engineering is to fabricate structures that deliver the appropriate bioactive molecule(s) for an extended period in a manner that effectively directs the regeneration of target tissue.[9] Microencapsulation of protein within a biodegradable polymer has been recognized as an attractive way to control the sustained delivery of bioactive molecules.[10,11] For instance, poly(D, L-lactic-co-glycolic acid) (PLGA) microspheres, because of their modestly-priced and reproducible fabrication processes, have been extensively studied for controlled sustained delivery of proteins.[12-14] PLGA microspheres' long-term degradation can facilitate release of bioactive molecule up to several months.[15,16] Further incorporating the bioactive molecule-loaded PLGA microspheres into a hydrogel structure has been shown to provide an added element of control to the release profile by mitigating the initial burst release that is often associated with the delivery either directly from Alg or other polymers alone.[2,17-20]

A number of structures have been fabricated and evaluated for their application in targeted local delivery of bioactive molecules for cell guidance through chemotaction.[21-23] In these applications, biofactor gradients within the structures provide chemotactic cues for directionally-guided cell growth and/or migration. However, these structures required highly complex technologies for fabrication and very few were able to generate a non-burst release profile that: i) effectively controlled delivery concentrations to those target cells/tissues, and ii) did not deliver most of the bioactive molecules in a very short period.

Fibrous structures have gained attention as bioactive molecule delivery systems. This is due to the simplicity of fabrication techniques as well as the large surface areas of the prepared fibres across which bioactive molecules are transported to the site of interest.[24] Electrospinning and wet spinning have been intensively explored to produce fibrous structures.[25-28] Wet-spinning is a non-solvent-induced phase inversion technique that is used to form continuous polymer microfibres by injecting the polymer solution into a coagulation bath composed of a poor solvent/solvent mixture with respect to the polymer. It has a potential advantage of converting biomaterials into fibres without the use of a high voltage, which may cause protein denaturation.[29] Wet-spinning can also produce filaments into complex geometries to address the needs for different bioactive molecule delivery applications.[30,31]

In this study, we present a simple and programmable approach for fabrication of Alg fibres containing protein-loaded microspheres. We incorporate the protein-loaded microspheres into the fibre structure to achieve sustained release of protein in a graduated manner conducive to chemotactic applications. This novel gradient fibre is specifically programmable in terms of the presence of bioactive molecules along the fibre length while also potentially providing a platform for directing cell growth.

Experimental section

Materials

Poly(D, L-lactide-co-glycolic acid) (PLGA, 50:50, inherent viscosity 0.4 dL/g (25 °C, 0.5 g/dL in $CHCl_3$)) was purchased from Corbion, Singapore. Alginic acid sodium salt from brown algae (Alg) (viscosity: 4-12 cP, 1 % in H_2O 25 °C), poly (vinyl alcohol) (PVA) (M_w 50,000–85,000 Da, 96% hydrolyzed), calcium chloride dihydrate, ethylenediaminetetraacetic acid (EDTA), sodium citrate and fluorescein isothiocyanate-conjugated bovine serum albumin (FITC-BSA) were all purchased from Sigma-Aldrich, Australia. Analytical grade dichloromethane (DCM) was obtained from Chem-Supply Pty Ltd, Australia. Milli-Q water (18 MΩ cm^{-1}) was used in the preparation of aqueous solutions. A simulated body fluid (SBF) solution, with ion concentrations equal to those of human blood plasma and primed with the following ion concentrations of 142 mM Na^+, 5 mM K^+, 1.5 mM Mg^{2+}, 2.5 mM Ca^{2+}, 103 mM Cl^-, 27 mM HCO_3^-, 1.0 mM HPO_4^{2-} and 0.5 mM SO_4^{2-} and with a pH adjusted to 7.4,[32] was used as the medium for the protein release study. EASYstrainer™ with a mesh size of 70 µm and Millex® Syringe sterile filters (pore size = 0.22 µm) were obtained from Greiner Bio-One (Austria) and MERCK (Germany), respectively.

Preparation of the protein-loaded PLGA microspheres

The PLGA microspheres were prepared via a modified water/oil/water (W/O/W) double-emulsion method. 1 g of PLGA was dissolved in 5 mL of DCM to form an oil phase (O). FITC-BSA, chosen as the model protein, was dissolved in Milli-Q water at 50 mg/ml concentration to obtain an inner aqueous phase (W1). The W1 was dispersed into an O phase by sonication (112 W, 5 min). The resulting primary emulsion (W1/O) was poured into 10 ml of 4% w/v aqueous PVA solution (as the outer aqueous phase (W2)) under sonication (112 W, 2 min). The whole suspension was then added to 250 ml of aqueous 0.4% w/v PVA solution and the

resulting double-emulsion was stirred at 1500 rpm for 2 h to evaporate the organic solvent. The PLGA microspheres were collected by centrifugation and washed with Milli-Q water three times. The final suspension of FITC-BSA-loaded PLGA microspheres in water was filtered using an EASYstrainer^{TM} with a mesh size of 70 µm. The microspheres were then freeze-dried and stored at -20 °C.

Wet spinning set-up and fabrication of Alg fibres with programmable loading of the protein-loaded PLGA microspheres

A customised spinning setup was developed involving two spinning dopes (Fig. 1). Spinning dope A, denoted as Alg spinning dope, was composed of 4%w/v Alg in water, and spinning dope B, denoted as Alg/PLGA spinning dope, was prepared by mixing 4% w/v Alg with the FITC-BSA-loaded PLGA microspheres at a weight ratio of Alg/PLGA = 3/2. The mixing procedure involved magnetic stirring of the Alg/PLGA spinning suspension for 5 min followed by ultrasonication for 2 min. The two spinning dopes were extruded via syringe A and B respectively, with the extrusion rates being controlled using a CM Printing System-LinuxCNC via a home-designed coded software. The two spinning dopes were mixed together in a mixing tube C (with the length of 39 mm and interior diameter of 3.5 mm) where a home-designed interior blender (with a diameter of 3.2 mm) was housed to facilitate the mixing of the two spinning dopes. The resultant final spinning dope was then injected into a coagulation bath containing an aqueous $CaCl_2$ solution (4% w/v). The coagulation bath was programmed to move at a predetermined speed of 50 $cm.min^{-1}$ in parallel to the direction of spinning to avoid any stress to the as-spun fibre.

To minimize the dead volume and waste of protein-loaded PLGA microspheres, the mixing tube C was prefilled with Alg spinning dope prior to the spinning process. Thus the as-spun

fibre contained an initial Alg-only part. The length of the Alg-only part can be calculated based on the extrusion rate of final spinning dope and the volume of the mixing tube C. At the completion of the spinning process, the initial Alg part was removed (at the cutting point shown in Fig. 1) to produce the desired fibre.

In this study, two types of microsphere-loaded Alg fibres were fabricated and characterized: Alg fibre with uniform distribution of the protein-loaded PLGA microspheres (U-Alg/PLGA fibre), and Alg fibre with a concentration gradient of protein-loaded PLGA microspheres (G-Alg/PLGA fibre). U-Alg/PLGA fibres were prepared by control of the extrusion rate ratio of the two spinning dopes, Alg spinning dope:Alg/PLGA spinning dope, at 1:1, using the procedure described above. Both Alg and Alg/PLGA spinning dopes were extruded at a fixed rate of 24 ml/h and mixed together to form the final spinning dope that was then extruded into the coagulation bath at a rate of 48 ml/h.

The G-Alg/PLGA fibres were produced using a similar procedure, but the ratio of extrusion rate of Alg spinning dope and Alg/PLGA spinning dope was programmed to vary linearly from 1:0 to 0:1 over a period of 15s. That is, the spinning procedure begun with an extrusion rate of 48 ml/h for Alg spinning dope, and 0 ml/h for Alg/PLGA spinning dope, and ended with an extrusion rate of 0 ml/h for Alg spinning dope and 48 ml/h for Alg/PLGA spinning dope. During the spinning process, the extrusion rate of the final spinning dope was fixed at 48 ml/h. By controlling the extrusion rate ratio of the two spinning dopes, a programmable loading of the protein-loaded PLGA microspheres in Alg fibres can be readily achieved.

For comparison, FITC-BSA-loaded Alg fibre (i.e. without prior encapsulation with PLGA) was also prepared using the same procedure as for U-Alg/PLGA fibres. To do so, spinning dope A

contained aqueous 4% w/v Alg solution and spinning dope B contained FITC-BSA dissolved in Alg solution 4% w/v (FITC-BSA/Alg, w/w, 1/90).

Rheological characterisation of the Alg spinning dopes

The rheological behaviour of the wet-spinning solutions was analysed using an AR-G2 rheometer (TA Instruments, New Castle, DE) equipped with a Peltier plate thermal controller. A 2º/36mm cone and plate geometry was used in all measurements. The solutions were held at 25 °C for 1 min prior to performing the experiments. Viscosity and shear stress were measured as a function of shear rate at 25 °C.

Morphological characterisation

Images of the as-spun and dried fibres were recorded by optical microscopy (Leica M205A, Austria). For scanning electron microscopy, the protein-loaded microspheres were mounted on metal stubs using conductive double-sided carbon tape and sputter-coated with a thin layer of gold (thickness = 15 nm). Microspheres diameters were analysed using Image J (n = 150). For longitudinal and cross-sectional imaging five sections of the hydrated G-Alg/PLGA fibre (at specific distances) were cut and inserted into pre-drilled holes (1 or 1.5 mm diameter) in a brass mounting block. The holes were of a depth which allowed fibres to be inserted upright and protrude from the surface. The block containing the mounted fibres was then plunged into liquid nitrogen for approximately 45 s and then the fibres were fractured using a liquid nitrogen cooled razor blade. The block was then quickly transferred to a LVSEM (JEOL JSM-6490 LV, Japan) for examination. Sample morphologies were then observed in secondary electron imaging mode at an accelerating voltage of 15 kV.

To confirm the presence and distribution of protein-loaded microspheres in the wet-spun fibres, the hydrated fibres were examined on a laser confocal scanning microscope (LCSM, Leica TCS SP2, Australia). The excitation and emission wavelengths used were 488 nm and 520 nm, respectively. Blank non-loaded Alg fibres were used as a negative control: firstly, to adjust all the parameters including the laser intensity and gain, until fluorescent signals could not be seen from the Alg fibre sample; then, without changing any settings, the same parameters were used to observe the fibres containing fluorescently labelled protein-loaded PLGA microspheres.

Fourier Transform Infrared Spectroscopy (FT-IR) and mechanical characterisation of the as-prepared fibres

The U-Alg/PLGA and G-Alg/PLGA fibres (air-dried at 20 ^{o}C) were characterized using an FT-IR spectrometer. The surface spectra were studied using an infrared microscope (AIM-8800, Shimadzu, Japan) in a reflectance mode equipped with a MCT (Mercury-Cadmium-Telluride) detector connected to the FT-IR instrument.

Tensile tests were carried out on a dynamic mechanical tester (EZ-L Tester from Shimadzu, Japan) at a strain rate of 0.1 cm.min^{-1} and a gauge length of 30 mm (n = 3). The tensile strength was calculated according to the formula, $\alpha = F/A$, where F is the maximum force (N) and A is the cross-sectional area (m^2) of the fibre, which is considered as the maximum stress in stress-strain curve of the fibres.[33] Moreover, elastic modulus of U-Alg/PLGA or G-Alg/PLGA fibres is defined as the ratio of tensile stress to tensile strain in the elastic part of the respective stress-strain curve.

Quantification of protein loading

For FITC-BSA-loaded PLGA microspheres, the microspheres (10 ~ 15 mg) were weighed and dissolved in 0.5 ml DCM and then 0.5 ml Milli-Q water was added. After vigorous agitation, the suspension was centrifuged (3000 rpm, 5 min) and a 200 μl sample from the aqueous phase was extracted for further analysis using a microplate reader at Ex_{max} = 485 nm and Em_{max} = 520 nm (the excitation and emission wavelengths, respectively). The protein loading (μg/mg microspheres) was quantified using a standard curve of fluorescence intensity vs FITC-BSA concentration. The results were expressed as mean ± standard deviation (n = 3).

For U-Alg/PLGA fibres, the fibres (length = 3 cm, n = 7) were weighed and dissolved in an aqueous solution containing EDTA (50 mM) and sodium citrate (100 mM).[8,34] After filtering the suspension, the remaining microspheres were washed with water to remove residual salt, dried at 37 °C and weighed. The result was expressed as mean ± standard deviation (n = 7). Based on the protein loading of the PLGA microspheres and mass of PLGA microspheres present in each fibre, the amount of protein loading in each fibre was calculated.

For G-Alg/PLGA fibres, the total protein loading in the fibres (length = 3 cm, n = 7) was determined using the same procedure as for U-Alg/PLGA fibres. In addition, to characterise the protein concentration gradient structure, the G-Alg/PLGA fibres (n = 7) were cut into half. Both the low protein-loading end and high protein-loading end were characterised for protein loading using the above method.

Protein Release Studies

Protein release studies from FITC-BSA-loaded PLGA microspheres, or Alg fibres with or without FITC-BSA-loaded PLGA microspheres were performed in SBF at 37 °C, with unloaded PLGA microspheres used as controls. Briefly, each sample was weighed and then

placed in 1.5 ml Eppendorf tubes with 300 µl of SBF and placed in an incubator shaker under slow shaking conditions. At each time point (0, 1, 3, 5, 7, 10, 14, 21, 28 and 35 days) the SBF supernatant was removed and replaced with fresh SBF and re-incubated until the next designated sampling time point. The released samples were stored at -20 °C and the protein content of the samples were quantified using a fluorescence microplate reader at Ex_{max} = 485 nm and Em_{max} = 520 nm (n = 3).

The premature protein release (i.e. protein released from the FITC-BSA-loaded microspheres during the mixing with the alginate prior to wet-spinning) was assessed. To do so, a mock wet-spinning process was followed (i.e. the extruded material did not interact with the coagulation bath). Briefly, 1 ml of alginate dope containing the FITC-BSA-loaded microspheres was extruded from the needle and collected. The sample was diluted 10 times, centrifuged and syringe filtered (pore size 0.22 µm). The filtered solution was again diluted 10 times and then assessed for protein content.

For G-Alg/PLGA fibres, in addition to monitoring the protein release as a function of time, the influence of the protein concentration gradient structure (Fig. 1c) on protein release was also assessed. The G-Alg/PLGA fibres (n = 7) were cut in half and both the low protein-loading end and high-protein loading ends were monitored for protein release as a function of time, using the same protocol as described for the FITC-BSA-loaded PLGA microspheres.

Results and Discussion

Preparation and characterisation of microspheres

The LVSEM image of the freeze-dried FITC-BSA-loaded PLGA microspheres and the confocal scanning microscopy image of the microspheres suspended in Alg spinning dope are

shown in Fig. 2. The microspheres prepared in this study exhibit smooth surfaces (Fig. 2a). The diameter of the microspheres ranged from 3 to 84 μm, with a mean size of ~ 25.8 μm. Fig. 2b shows that the FITC-BSA-loaded PLGA microspheres were well dispersed in the Alg spinning dope, with no observable agglomeration. Fig. 2c shows the size distribution of the protein-loaded PLGA microspheres. The encapsulation efficiency of FITC-BSA into the PLGA microspheres was ~ 61.0 ± 8.9%.

Rheological characterisation of the Alg spinning dopes

The study of the rheological behaviour of spinning dopes is critical for production of a wet-spun product. For co-spinning of multiple-component dopes, matching the rheology of the components is also important; any non-compliance in rheology of the two dopes will result in poor mixing of spinning dopes, and subsequently, formation of inhomogeneous final spinning dope that leads to poor quality wet-spun fibres.

Under shear, Alg polymer chains are in a less expanded conformation and become less entangled causing their viscosity to fall. Fig. 3a and 3b show the variations in viscosity and shear stress for Alg and Alg/PLGA spinning dopes as a function of shear rate, respectively. To extrude the Alg spinning dopes through a needle/spinneret to form microfibres, the viscosity of the dope should be typically in the range of 0.01-2 Pa.s versus the shear rate range of 1-100 1/s.[35,36] The presence of PLGA microspheres caused slight variations (≤ 0.4 Pa.s) in the rheological behaviour of Alg/PLGA spinning dope but both dopes remained fairly constant as the shear rate increased. Considering the relatively similar rheological behaviour of these two spinning dopes (under the supposed shear rate range for wet-spinning), it is expected that they should be well-mixed.

Morphological characterisation of the as-prepared fibres

Visual inspection of the U-Alg/PLGA fibres showed a smooth surface morphology and that FITC-BSA-loaded microspheres are uniformly distributed inside the fibres (Fig. 4a and 4b). This structure could be attributed to the difference between the interior diameter of the mixing tube C (d = 3.5 mm) and the blender's diameter (d = 3.2 mm) (Fig. 1b). As previously mentioned, prior to the spinning process, the mixing tube was initially filled with the Alg spinning dope, and through the spinning process, the blender mixed the two extruded spinning dopes in the middle of the tube. This can produce a final spinning dope bearing an outer thin layer of Alg, which then resulted in wet-spun fibres with an Alg coating. This view is supported by our FT-IR spectroscopy characterisation which is discussed in the next section.

We studied the morphology of G-Alg/PLGA fibres to investigate the gradient structure. Fig. 5a shows the longitudinal LVSEM image of a hydrated G-Alg/PLGA fibre at the high protein-loading end, and Fig. 5b and 5c show the schematic and the longitudinal optical image of G-Alg/PLGA fibre, respectively. The G-Alg/PLGA fibre, like U-Alg/PLGA fibres, has a relatively smooth surface morphology even in the region with the highest concentration of microspheres (Fig. 5a inset). This microsphere concentration gradient structure of the G-Alg/PLGA fibre can be observed in Fig. 5c. Fig. 5i-5v represent the cross-sectional LVSEM images of hydrated G-Alg/PLGA fibre at 5 different points (specified in Fig. 5c). Fig. 5iv-a is a closer view of the central part of Fig. 5iv. These images present the distribution of microspheres inside the fibre structure. The laser confocal scanning image of G-Alg/PLGA fibre shows the gradient distribution of the fluorescently labelled microspheres (green, Fig. 5d), which is characterised by the intensity mapping of the green fluorescence that increases progressively from the right-hand end (low concentration of microspheres) to the left-hand end of the fibre (high concentration of microspheres). On closer observation (Fig. 5d-a, 5d-b, 5d-c

and 5d-d), it is evident that the number of microspheres in the four insets increases from right to left.

Fourier Transform Infrared Spectroscopy (FT-IR) and mechanical characterisation of the as-prepared fibres

For G-Alg/PLGA fibres, FT-IR spectra were recorded at five distinct sections from the low protein concentration end to the high protein concentration end. Our results showed no discernible difference in the spectra gathered at these positions (data not shown). Furthermore, both U-Alg/PLGA and G-Alg/PLGA fibres showed almost similar spectra as those of pure alginate, indicating the presence of alginate structure at the fibre surface (Fig. 6). The major peaks in the characteristic spectra of alginate can be observed at 2924 cm^{-1} and 1405 cm^{-1} due to stretching $–CH_2$ and the carboxylic groups, respectively. Moreover, the peak at 1594 cm^{-1} indicates the asymmetric stretch of C–O–H. Other main peaks attributed to the Alg are seen at 3311 cm^{-1} and 1120 cm^{-1}, corresponding to the stretching vibration of O–H and stretching vibration of secondary alcohol (CH–OH), respectively.[37-38] Minor peaks at 1754 cm^{-1} and 1161 cm^{-1} were noted in both spectra, which are associated with the carbonyl bond C=O stretching vibration and the C–O stretching, respectively, both of which are characteristic of PLGA.[39,40]

The mechanical properties of the U-Alg/PLGA and G-Alg/PLGA fibres were investigated to assess the effect of the distribution gradient of the FITC-BSA-loaded PLGA spheres on the final properties of these fibres. All the fibres were cut into 3 cm long pieces for this testing. Fig. 7 and Table 1 show the mechanical properties of air-dried fibres. U-Alg/PLGA and G-Alg/PLGA fibres showed typical alginate fibre structure behaviour (while undergoing stress) by displaying an extra elongation before breaking completely (highlighted with the light grey dashed box in Fig. 7).[41] G-Alg/PLGA fibres exhibit a lower mechanical strength compared

with U-Alg/PLGA fibres, which might be related to the non-uniform gradient distribution of the microspheres along the G-Alg/PLGA fibres.

Protein release study

Firstly, the FITC-BSA release profiles of the protein-loaded PLGA microspheres and Alg fibres were assessed to investigate the effect of both PLGA and alginate encapsulation on protein release. FITC-BSA-loaded PLGA microspheres showed a continued release for more than 35 days, with ~55% of the loaded protein being released within the observed period (Fig. 8a). *In vitro* degradation study was undertaken by monitoring mass loss of the microspheres at various time intervals. Significant weight loss was noted only after two weeks' incubation (~3% at week 2, ~12% at week 3, and ~23% at week 5). This result is consistent with those previously reported,[42] and suggested that the protein release kinetics of the PLGA microspheres was predominantly diffusion-controlled in the first two weeks of release study, after which polymer degradation played an increasing role in modulating the release profile of the microspheres. By contrast, FITC-BSA directly encapsulated into Alg fibres shows a rapid release, with ≥ ~44% released at day 1 and ~70% at day 5. The 2nd week saw only ~1% protein being released from day 7 to day 10, after which no more released protein could be detected.

The FITC-BSA release profile of U-Alg/PLGA and G-Alg/PLGA fibres are also presented in Fig. 8a. Both U-Alg/PLGA and G-Alg/PLGA fibres were designed to contain 20 wt% of protein-loaded PLGA microspheres and the practical protein loadings in U-Alg/PLGA and G-Alg/PLGA fibres are reported in Table 2. Both fibres showed similar release profiles, with much reduced initial burst release at day 1 (~6% for both fibres). The amount of protein released by day 5 is ~23% of the total loading, after which a progressive reduction in the amount of protein released is noted. The cumulative amount of protein released is ~28% of the

total loading by day 15, and ~32% of the total loading by day 35 following a further reduction in the protein release rate after day 15.

It is shown in Fig. 8a that the initial amounts of protein released from both fibres (≤ day 5) are close to that from the FITC-BSA-loaded PLGA microspheres alone. This, however, may be due to the premature release of protein from the microspheres prior to the solidification of fibres. To support this, we have assessed the amount of premature protein release, which revealed that ~6.1±4.2% of loaded protein was released into the spinning dope prior to the fibre formation. As shown in Fig. 8a, the protein release from U-Alg/PLGA or G-Alg/PLGA fibres after day 5 become much slower than the FITC-BSA-loaded PLGA microspheres or the FITC-BSA-loaded Alg fibres alone. Fig. 8b provides a closer view of the protein release profiles from these two fibres at a later stage following day 5. Rather than reaching a plateau after 15 days, both fibres exhibit a further reduced, progressive release for more than 35 days. This supports the view that incorporation of FITC-BSA loaded microspheres into an Alg fibrous matrix facilitates realisation of a more extended protein release profile. This is probably due to limited interactions between the encapsulated spheres and surrounding release medium and consequently reduced degradation kinetics as a result of alginate encapsulation.

Similar studies by others provide some insight into the protein release profiles observed with U-Alg/PLGA and G/Alg/PLGA fibres. Alsmadi et al.[21] developed a nerve growth factor (NGF) loaded gradient structure within agarose microchannels. The structure was shown *in vitro* to be able to direct sensory axonal growth along NGF gradients. However, in terms of NGF release, the structure showed a large burst release at day 1 and completion of release by day 7. Johnson et al.[43] developed 3D-printed nerve pathways to deliver NGF and glial cell line-derived neurotrophic factor in a gradient fashion. The bioactive molecules were directly loaded in a

modified gelatin hydrogel matrix. Completion of protein release was achieved in 21 days. Compared with the findings reported by Alsmadi and Johnson, incorporation of protein-loaded PLGA microspheres into an Alg fibrous matrix in a uniform or gradient manner results in much sustained release suitable for longer term release applications.

We also studied the release profile of the two half sections of G-Alg/PLGA fibre (low protein-loading end and high protein-loading end, as specified in Fig. 5b). The low protein-loading end has a practical microspheres loading of ~ 28.6% of the total mass, and the high protein-loading end has a practical microspheres loading of ~ 69.2% of the total mass. As shown in Fig. 8d, like G-Alg/PLGA fibre, both the low protein-loading end and the high protein-loading end showed an initial slight burst release followed by a continuous release until day 10. Their release rates then became much slower until the end of the observation period (35 days). The high protein-loading end demonstrated a faster release rate, during the first 10 days, than the low protein-loading end. It seems that with increased concentration of microspheres, the Alg component in the resultant fibres is reduced, presenting, to a lesser degree, a diffusion barrier to the protein release. This suggests that the concentration of protein along the fibres can be spatiotemporally regulated by modulating the gradient distribution of protein-loaded microspheres within the structure.

There are some other delivery configurations reported in recent years, which are capable of providing guidance (directing) platforms. For instance, Ostrovidov et al.[22] used a microfluidic gradient generator to develop a microengineered hydrogel with a concentration gradient of okadaic acid for high-throughput analysis of drug-cell interactions. The drug was released from the hydrogel in a gradient manner and resulted in a gradient of cell viability. Although most of the gradient platforms reported to date could successfully deliver factors of interest in a specific

direction, they required complicated fabrication processes for achieving the gradient structure.[21, 23] In addition, they displayed a rapid release profile with completion of release over a short period of few days.[21,22,41-45] In contrast, the two-phase Alg fibre structure containing FITC-BSA-loaded PLGA microspheres presented here allows construction of a protein concentration gradient and delivery over a sustained period, which cannot be achieved with PLGA microspheres or Alg fibre alone.

Conclusions

In this study, we present a technique for fabrication of a two-phase Alg/PLGA fibre protein delivery system. FITC-BSA (a model protein) is encapsulated in PLGA microspheres and then incorporated into an Alg fibre structure via a custom-designed programmable wet-spinning method. The process demonstrates reliable production of Alg fibre with controlled presentation of the embedded protein. In particular, the system has demonstrated the capability to facilitate fibres that contained a defined microsphere concentration gradient that could be readily varied/tailored according to specific release requirements for the protein species in question. These fibres showed a more sustained release profile of protein than the protein-loaded PLGA microspheres or Alg fibres alone. The concentration gradient aspect of the two-phase Alg/PLGA fibre system presented here provides the possibility of guided chemotaxis by gradual presentation of cytokines or other growth factors in a spatially directional manner along a fibre. This has exciting potential for the applications in the promotion and direction of guided tissue regeneration in “linear” systems such as muscle and nerve. En route to this, further studies are required, such as incorporation of growth factor(s) of interest and optimization of gradient presentation of the growth factor(s) in terms of directing cell growth and differentiation.

Conflicts of interest

There are no conflicts of interest to declare.

Acknowledgements

Funding from the Australian Research Council Centre of Excellence Scheme (Project Number CE 14100012) is gratefully acknowledged. Gordon G. Wallace is grateful to the ARC for support under the Australian Laureate Fellowship scheme (FL 110100196). The authors also gratefully acknowledge the use of facilities within the Electron Microscopy Centre (EMC) and the Australian National Fabrication Facility (ANFF). Finally, the authors thank Associate Professor Chee O. Too for proofreading this manuscript.

References

1. M. S. Hamid Akash, K. Rehman and S. Chen, *Polymer Reviews*, 2015, **55**, 371-406.
2. K. Wanawananon, S. E. Moulton, G. G. Wallace and S. Liawruangrath, *Polymers for Advanced Technologies*, 2016, **27**, 1014-1019.
3. M. Sheikhpour, L. Barani and A. Kasaeian, *Journal of Controlled Release*, 2017, **253**, 97-109.
4. D. H. Choi, C. H. Park, I. H. Kim, H. J. Chun, K. Park and D. K. Han, *Journal of Controlled Release*, 2010, **147**, 193-201.
5. X. Wei, C. Gong, M. Gou, S. Fu, Q. Guo, S. Shi, F. Luo, G. Guo, L. Qiu and Z. Qian, *International Journal of Pharmaceutics*, 2009, **381**, 1-18.
6. V. Andrés-Guerrero, M. Zong, E. Ramsay, B. Rojas, S. Sarkhel, B. Gallego, R. de Hoz, A. I. Ramírez, J. J. Salazar, A. Triviño, J. M. Ramírez, E. M. del Amo, N. Cameron, B. de-las-Heras, A. Urtti, G. Mihov, A. Dias and R. Herrero-Vanrell, *Journal of Controlled Release*, 2015, **211**, 105-117.
7. A. Lengalova, A. Vesel, Y. Feng and V. Sencadas, *International Journal of Polymer Science*, 2016, **Article ID 6047284**, 1-2.
8. A. Sosnik, *ISRN Pharmaceutics*, 2014, **Article ID 926157**, 1-17.
9. T. J. Whitehead and H. G. Sundararaghavan, *Journal of Visualized Experiments*, 2014, **90**, 51517-51525.
10. C. Tomaro-Duchesneau, S. Saha, M. Malhotra, I. Kahouli and S. Prakash, *Journal of Pharmaceutics*, 2013, **Article ID 103527**, 1-19.
11. G. Ma, *Journal of Controlled Release*, 2014, **193**, 324-340.
12. F. Ramazani, W. Chen, C. F. van Nostrum, G. Storm, F. Kiessling, T. Lammers, W. E. Hennink and R. J. Kok, *International Journal of Pharmaceutics*, 2016, **499**, 358-367.
13. Z. Liu, X. Li, B. Xiu, C. Duan, J. Li, X. Zhang, X. Yang, W. Dai, H. Johnson, H. Zhang and X. Feng, *Colloids and Surfaces B: Biointerfaces*, 2016, **145**, 679-687.

14. K. Tajdaran, T. Gordon, M. D. Wood, M. S. Shoichet and G. H. Borschel, *Journal of Biomedical Materials Research Part A*, 2016, **104**, 367-376.
15. H. Gu, C. Song, D. Long, L. Mei and H. Sun, *Polymer International*, 2007, **56**, 1272-1280.
16. A. Giteau, M. C. Venier-Julienne, S. Marchal, J. L. Courthaudon, M. Sergent, C. Montero-Menei, J. M. Verdier and J.-P. Benoit, *European Journal of Pharmaceutics and Biopharmaceutics*, 2008, **70**, 127-136.
17. H. Kaygusuz, M. Uysal, V. Adımcılar and F. B. Erim, *Journal of Bioactive and Compatible Polymers*, 2015, **30**, 48-56.
18. R. Wongkanya, P. Chuysinuan, C. Pengsuk, S. Techasakul, K. Lirdprapamongkol, J. Svasti and P. Nooeaid, *Journal of Science: Advanced Materials and Devices*, 2017, **2**, 309-306.
19. G. J. S. Dawes, L. E. Fratila-Apachitei, B. S. Necula, I. Apachitei, G. J. Witkamp and J. Duszczyk, *Journal of Materials Science. Materials in Medicine*, 2010, **21**, 215-221.
20. P. Zhai, X.b. Chen, D.J. Schreyer, *Materials Science and Engineering: C*, 2015, **56**, 251-259.
21. N. Z. Alsmadi, L. S. Patil, E. M. Hor, P. Lofti, J. M. Razal, C. J. Chuong, G. G. Wallace and M. I. Romero-Ortega, *Brain Research*, 2015, **1619**, 72-83.
22. S. Ostrovidov, N. Annabi, A. Seidi, M. Ramalingam, F. Dehghani, H. Kaji and A. Khademhosseini, *Analytical Chemistry*, 2012, **84**, 1302-1309.
23. J. L. Roam, P. K. Nguyen and D. L. Elbert, *Biomaterials*, 2014, **35**, 6473-6481.
24. Z. Yazhe, M. Pyda and P. Cebe, *Journal of Applied Polymer Science*, 2017, **134**, 1-9.
25. K. Kim, Y. K. Luu, C. Chang, D. Fang, B. S. Hsiao, B. Chu and M. Hadjiargyrou, *Journal of Controlled Release*, 2004, **98**, 47-56.
26. C. Li, C. Vepari, H.J. Jin, H. J. Kim and D. L. Kaplan, *Biomaterials*, 2006, **27**, 3115-3124.
27. D. Puppi, C. Mota, M. Gazzarri, D. Dinucci, A. Gloria, M. Myrzabekova, L. Ambrosio and F. Chiellini, *Biomed Microdevices*, 2012, **14**, 1115-1127.
28. K. Tuzlakoglu, I. Pashkuleva, M. T. Rodrigues, M. E. Gomes, G. H. van Lenthe, R. Müller and R. L. Reis, *Journal of Biomedical Materials Research Part A*, 2010, **92A**, 369-377.
29. D. Puppi and F. Chiellini, *Polymer International*, 2017, **66**, 1690-1696.
30. D. Puppi, D. Dinucci, C. Bartoli, C. Mota, C. Migone, F. Dini, G. Barsotti, F. Carlucci and F. Chiellini, *Journal of Bioactive and Compatible Polymers*, 2011, **26**, 478-492.
31. J. M. Razal, M. Kita, A. F. Quigley, E. Kennedy, S. E. Moulton, R. M. I. Kapsa, G. M. Clark and G. G. Wallace, *Advanced Functional Materials*, 2009, **19**, 3381-3388.
32. S. A. Martel-Estrada, C. A. Martínez-Pérez, J. G. Chacón-Nava, P. E. García-Casillas and I. Olivas–Armendáriz, *Materials Letters*, 2011, **65**, 137-141.
33. F. Mehrpouya, J. Foroughi, S. Naficy, J.M. Razal, M. Naebe, *Nanomaterials*, 2017, **7**, 293-304.
34. A. Saravana Kumar, P. Renuka Devi and K. R. Mani, *Asian Journal of Chemistry*, 2011, **23**, 3279-3282.
35. Y. Qin, *Polymer International*, 2008, **57**, 171-180.
36. J. M. Dealy and K. F. Wissbrun, in *Melt Rheology and Its Role in Plastics Processing: Theory and Applications*, *Springer Netherlands*, *Dordrecht*, 1999, 441-490.
37. B. Palma Santana, F. Nedel, E. Piva, R. Varella de Carvalho, F. Fernando Demarco, *BioMed Research International*, 2013, **Article ID 307602**, 1-6.
38. J. Zhang, Q. Ji, X. Shen, Y. Xia, L. Tan and Q. Kong, *Polymer Degradation and Stability*, 2011, **96**, 936-942.

39. C. C. Moura, M. A. Segundo, J. Das Neves, S. Reis and B. Sarmento, *International Journal of Nanomedicine*, 2014, **9**, 4911-4922.
40. Y. Ma, Y. Zheng, K. Liu, G. Tian, Y. Tian, L. Xu, F. Yan, L. Huang and L. Mei, *Nanoscale Research Letters*, 2010, **5**, 1161–1169.
41. J. Foroughi, G. M. Spinks and G. G. Wallace, *Journal of Materials Chemistry*, 2011, **21**, 6421-6426.
42. O. Karal-Yilmaz, M. Serhati, K. Baysal, B. M. Baysal, *Journal of Microencapsulation*, 2011, **28**, 46-54.
43. B. N. Johnson, K. Z. Lancaster, G. Zhen, J. He, M. K. Gupta, Y. L. Kong, E. A. Engel, K. D. Krick, A. Ju, F. Meng, L. W. Enquist, X. Jia and M. C. McAlpine, *Advanced functional materials*, 2015, **25**, 6205-6217.
44. P. J. Johnson, S. L. Skornia, S. E. Stabenfeldt and R. K. Willits, *Journal of Biomedical Materials Research Part A*, 2008, **86A**, 420-427.
45. T. A. Kapur and M. S. Shoichet, *Journal of Biomedical Materials Research Part A*, 2004, **68A**, 235-243.

Fig. 1 (a) Schematic of the novel programmable wet-spinning technology. The extrusion rates of Alg spinning dope (in syringe A) and Alg/PLGA spinning dope (in syringe B) are adjusted using a CM Printing System-LinuxCNC via a home-designed coded software. The two spinning dopes were mixed in a mixing tube C to form the final spinning dope. Then the final dope was extruded through a needle to form a fibrous structure. (b) A closer view of the mixing tube C, where a small flexible blender was inserted to facilitate the mixing of the two spinning dopes. (c) Schematic illustration of U-Alg/PLGA and G-Alg/PLGA fibres produced using the above procedure.

Fig. 2 (a) LVSEM image of the freeze-dried FITC-BSA-loaded PLGA microspheres, (b) laser confocal scanning microscopy image of the FITC-BSA-loaded PLGA microspheres dispersed in Alg spinning dope, and (c) size distribution of the as-prepared protein-loaded PLGA microspheres.

Fig. 3 (a) Viscosity and (b) shear stress of Alg and Alg/PLGA spinning dopes.

Fig. 2 Images of the as-spun U-Alg/PLGA. (a) is the optical image (depth of focus = 240 μm), and (b) is LVSEM image. Scale bars = 500 μm.

Fig. 5 (a) The longitudinal LVSEM image of high protein-loading end of G-Alg/PLGA fibre. (b) Schematic and (c) optical image of G-Alg/PLGA fibre. (i)-(v) are the cross-sectional LVSEM images, samples taken at five different points as specified in (c) from low protein-loading end i to high protein-loading end v of G-Alg/PLGA. (iv-a) is a higher magnification LVSEM image of iv. (d) is the longitudinal laser confocal scanning microscopy image of a representative G-Alg/PLGA fibre. (d-a), (d-b), (d-b) and (d-d) are closer views of the four different points as specified along the G-Alg/PLGA fibre.

Fig. 6 FT-IR spectra of Alg, U-Alg/PLGA and G-Alg/PLGA fibres and FITC-BSA-loaded PLGA microspheres.

Fig. 3 Stress-strain curves of U-Alg/PLGA and G-Alg/PLGA fibres. The dashed box highlights the extra elongation before the complete breakage of the fibres while undergoing stress.

Fig. 8 (a) A comparison of the release profile from PLGA microspheres, Alg fibre, U-Alg/PLGA and G-Alg/PLGA fibres. (b) A closer view of the FITC-BSA release profile of U-Alg/PLGA and G-Alg/PLGA fibres from day 5 to day 35. (c) A comparison of the release profile from G-Alg/PLGA fibre, the low protein-loading end of the G-Alg/PLGA fibre and the high protein-loading end of the G-Alg/PLGA fibre.

Table 1 Mechanical properties of Alg wet-spun fibres containing BSA-FITC-loaded PLGA spheres.

Sample	Mean diameter of as-spun fibres(μm)	Mean diameter of dried fibres (μm)	Elastic Modulus (MPa)	Tensile Strength (MPa)	Tensile Strain at break (%)
U-Alg/PLGA	567±14	368±11	9.5	12.4±3.2	6.8±0.6
G-Alg/PLGA	588±19	379±12	9.5	10.6±1.8	8.8±0.9

Table 2 Protein loading in PLGA microspheres and Alg/PLGA fibres.

Samples	FITC-BSA loaded PLGA microspheres	U-Alg/PLGA fibre	G-Alg/PLGA fibre	Low protein-loading end	High protein-loading end
FITC-BSA loading (μg/mg of the fabricated structure)	15.2	3.0	3.0	1.9	3.9

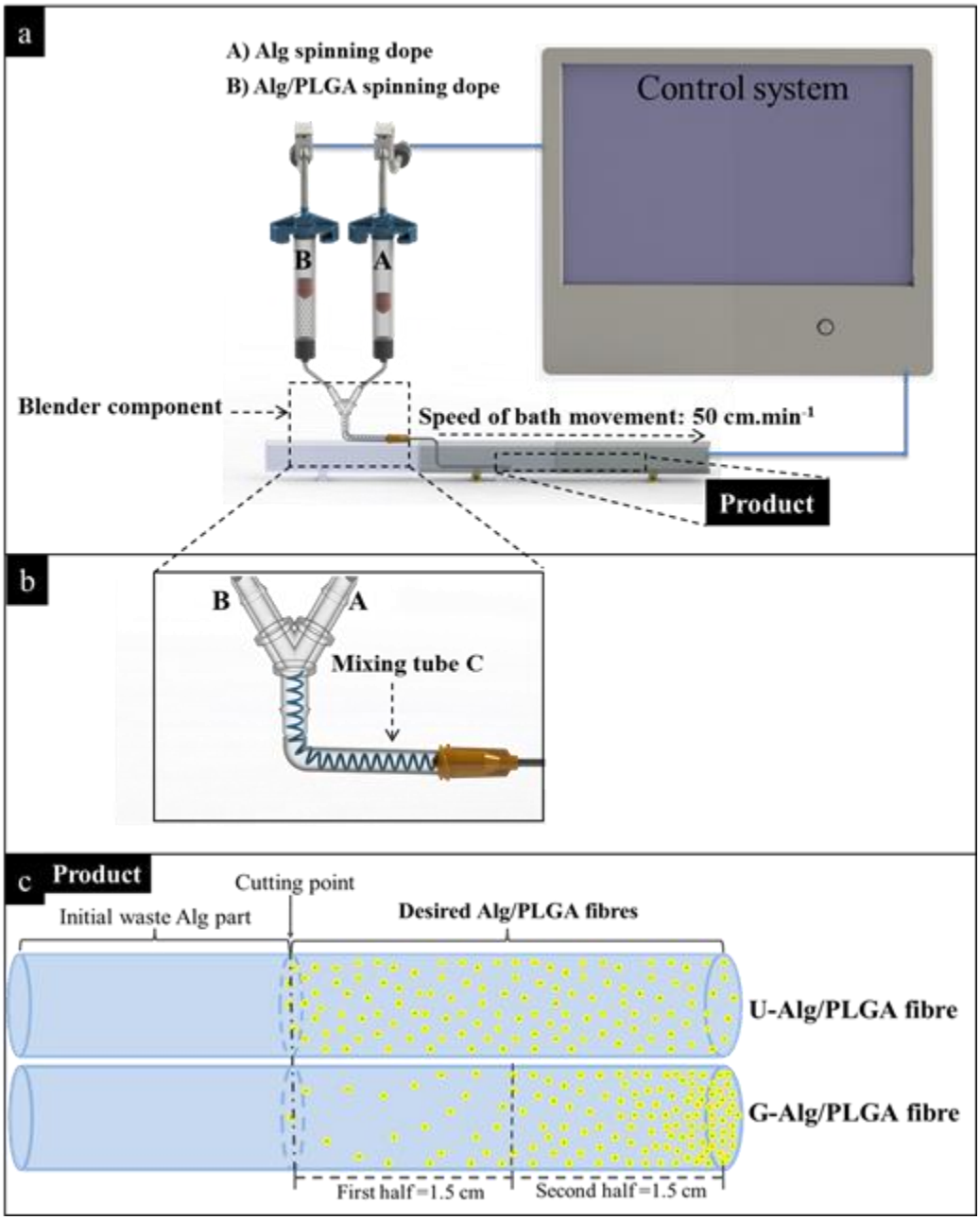
a
A) Alg spinning dope
B) Alg/PLGA spinning dope
Control system
B
A
Blender component
Speed of bath movement: 50 cm.min-1
Product
b
B
A
Mixing tube C
c
Product
Cutting point
Initial waste Alg part
Desired Alg/PLGA fibres
U-Alg/PLGA fibre
G-Alg/PLGA fibre
First half =1.5 cm
Second half =1.5 cm

Fig. 1

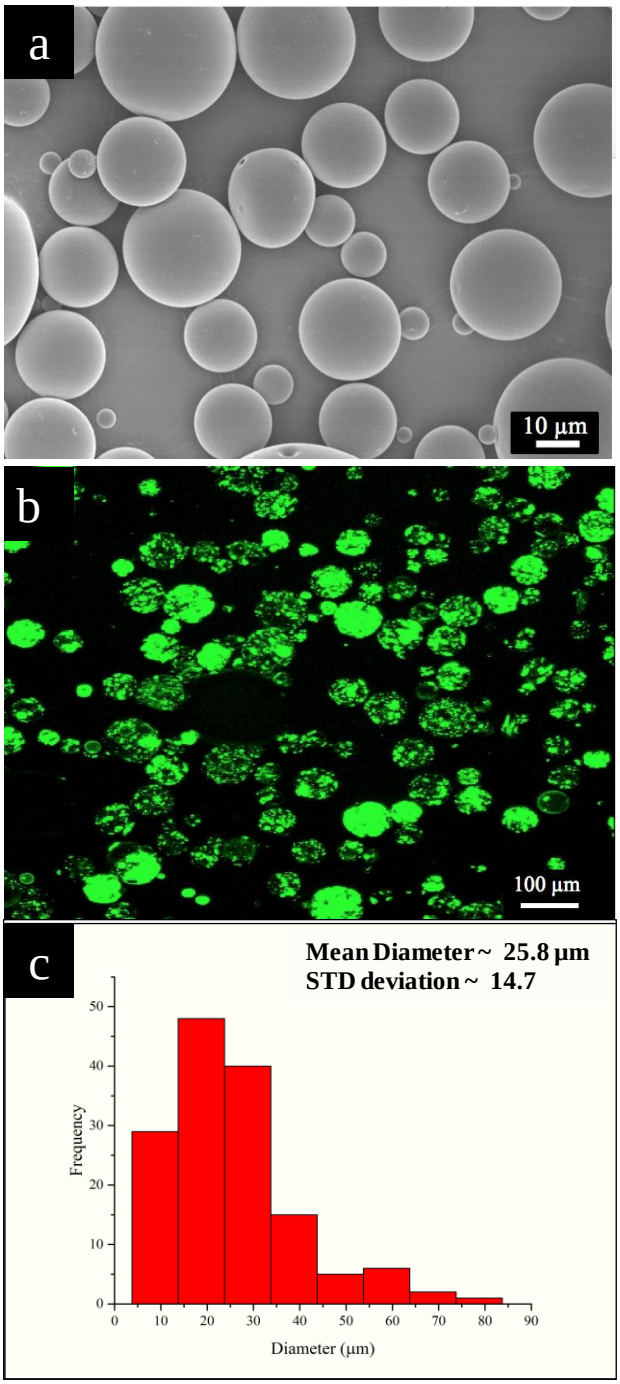
a
10 µm
b
100 µm
c
Mean Diameter ~ 25.8 µm
STD deviation ~ 14.7
Frequency
Diameter (µm)
0
10
20
30
40
50
60
70
80
90

Fig. 2

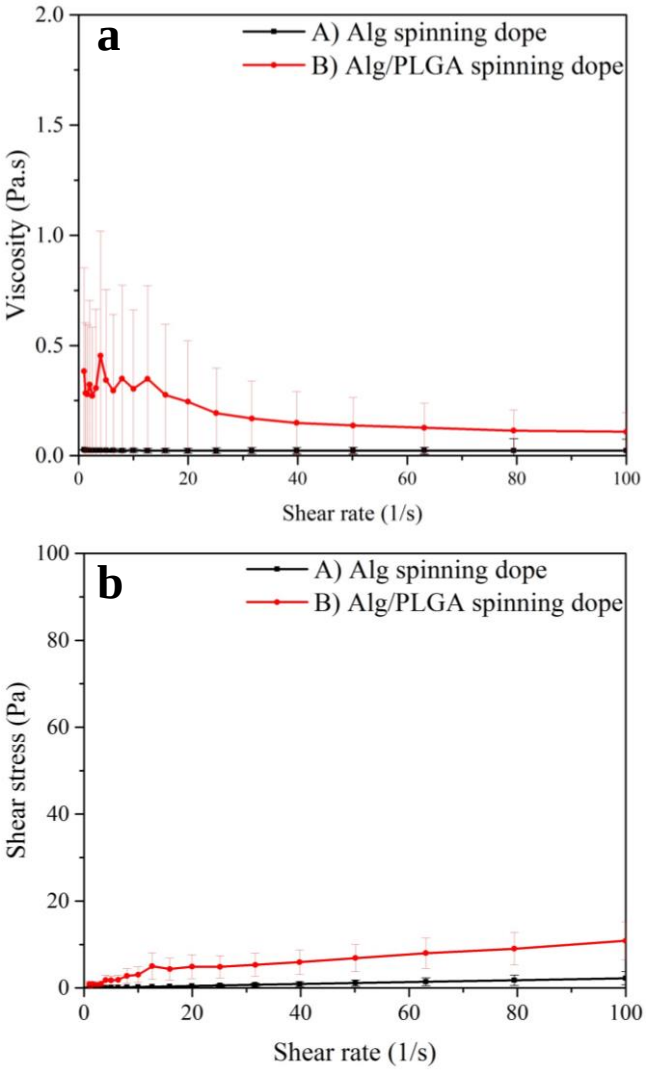
a
A) Alg spinning dope
B) Alg/PLGA spinning dope
Viscosity (Pa.s)
Shear rate (1/s)
b
A) Alg spinning dope
B) Alg/PLGA spinning dope
Shear stress (Pa)
Shear rate (1/s)

Fig. 3

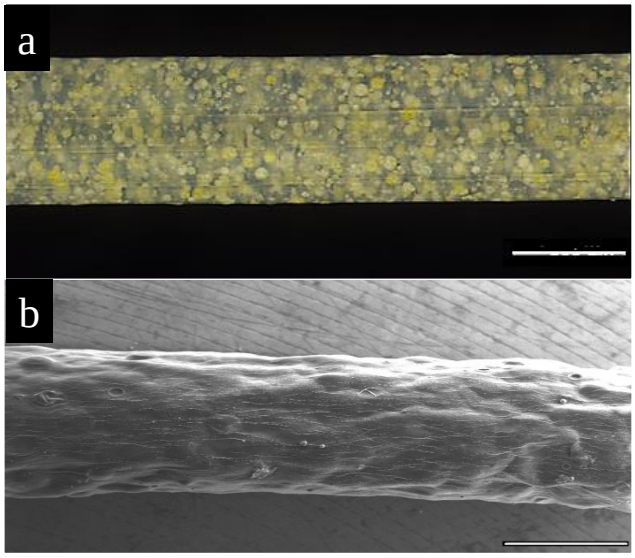

Fig. 4

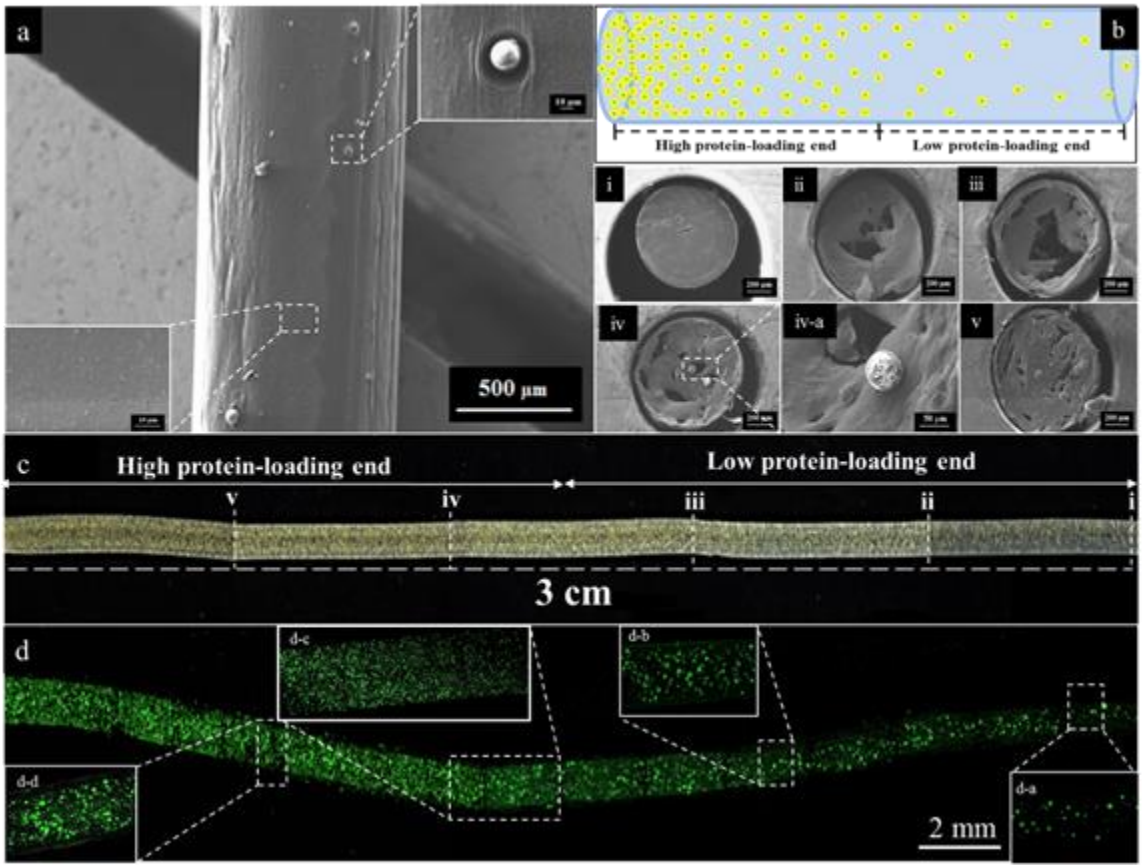
a
500 μm
b
High protein-loading end
Low protein-loading end
i
ii
iii
iv
iv-a
v
c
High protein-loading end
Low protein-loading end
v
iv
iii
ii
i
3 cm
d
d-c
d-b
d-d
d-a
2 mm

Fig. 5

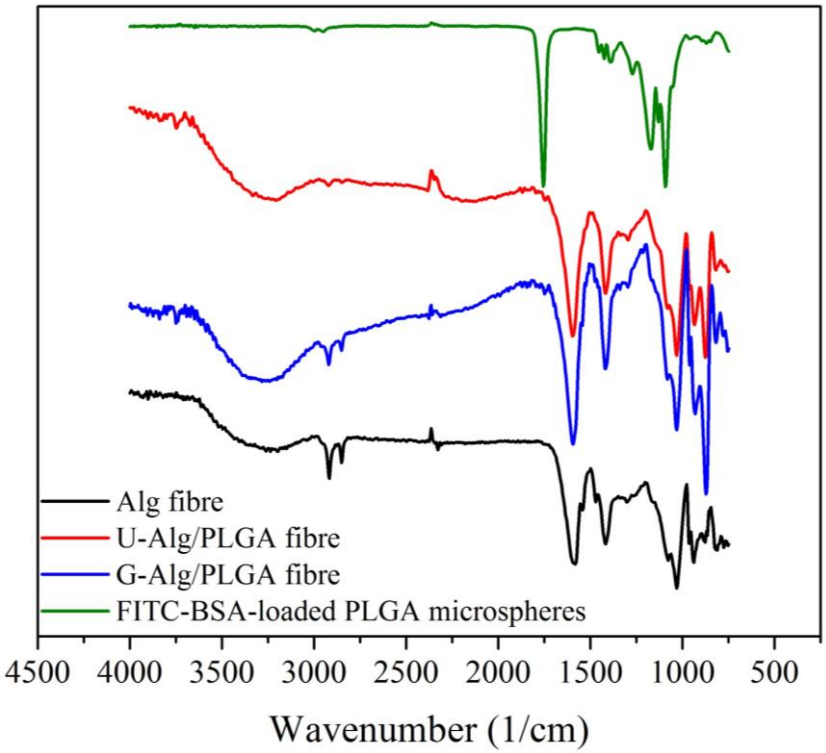
Alg fibre
U-Alg/PLGA fibre
G-Alg/PLGA fibre
FITC-BSA-loaded PLGA microspheres
4500
4000
3500
3000
2500
2000
1500
1000
500
Wavenumber (1/cm)

Fig. 6

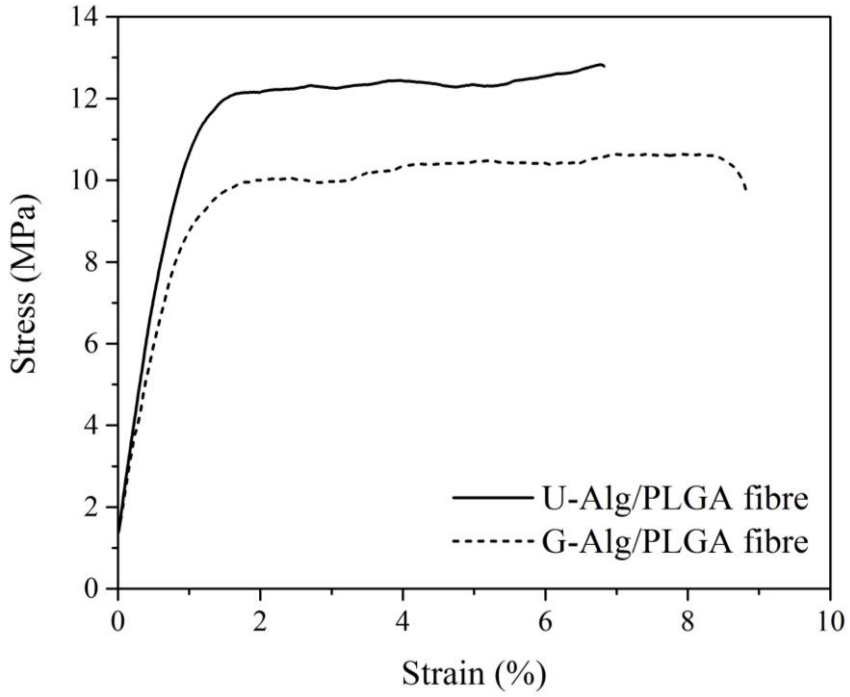
Stress (MPa)
Strain (%)
U-Alg/PLGA fibre
G-Alg/PLGA fibre
0
2
4
6
8
10
12
14

Fig. 7

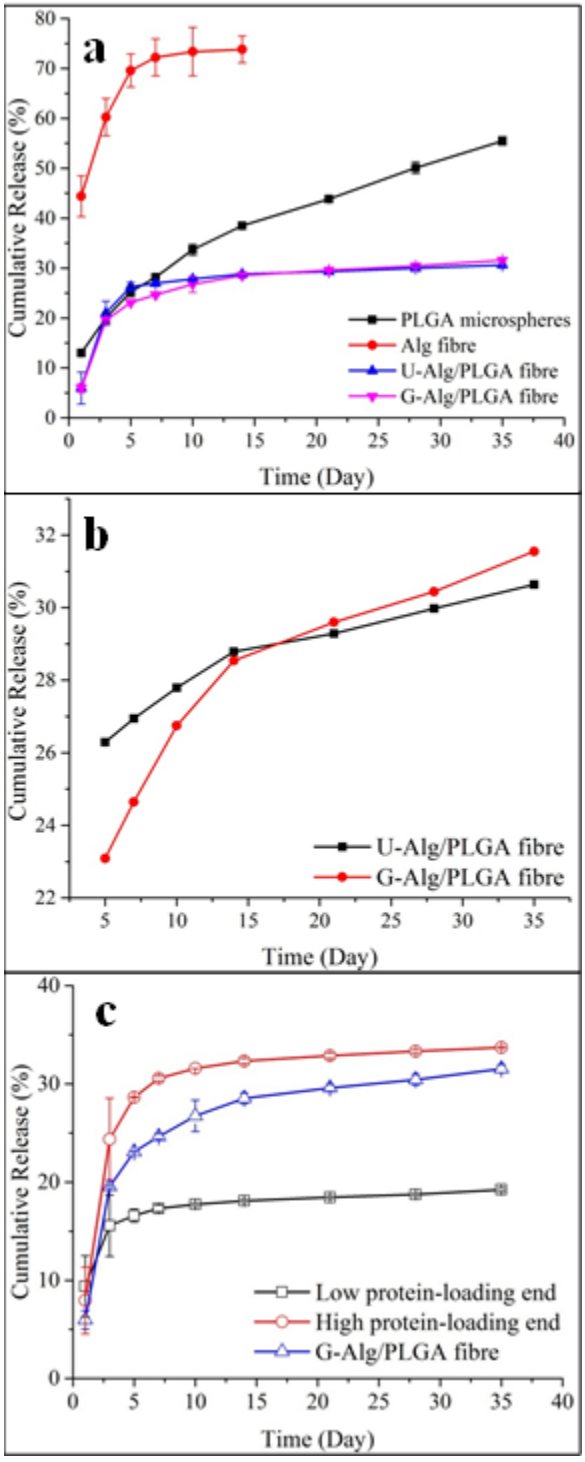
a
Cumulative Release (%)
Time (Day)
PLGA microspheres
Alg fibre
U-Alg/PLGA fibre
G-Alg/PLGA fibre
b
Cumulative Release (%)
Time (Day)
U-Alg/PLGA fibre
G-Alg/PLGA fibre
c
Cumulative Release (%)
Time (Day)
Low protein-loading end
High protein-loading end
G-Alg/PLGA fibre

Fig. 8

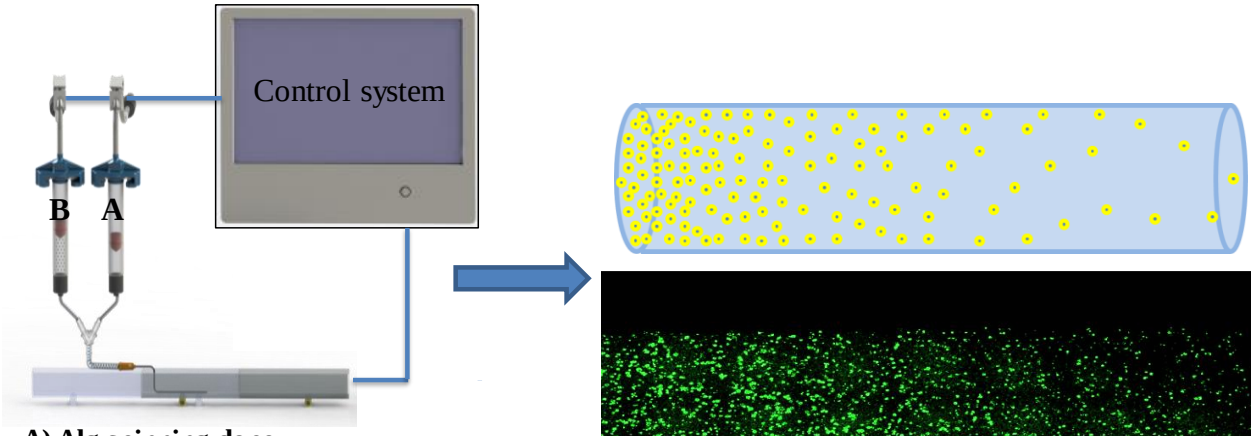

A) Alg spinning dope

B) Alg/PLGA spinning dope

Herein we present a simple approach for fabrication of alginate fibers with programmable microsphere concentration gradients for local protein delivery.

TOC